Role of Asp193 in Chromophore-Protein Interaction of *pharaonis* Phoborhodopsin (Sensory Rhodopsin II)

Masayuki Iwamoto,* Yuji Furutani,† Yuki Sudo,* Kazumi Shimono,* Hideki Kandori,† and Naoki Kamo*
*Laboratory of Biophysical Chemistry, Graduate School of Pharmaceutical Sciences, Hokkaido University, Sapporo 060-0812, Japan, and †Department of Biophysics, Graduate School of Science, Kyoto University, Sakyo-ku, Kyoto 606-8502, Japan

ABSTRACT *Pharaonis* phoborhodopsin (*p*pR; also *pharaonis* sensory rhodopsin II, psRII) is a receptor of the negative phototaxis of *Natronobacterium pharaonis*. By spectroscopic titration of D193N and D193E mutants, the pK_a of the Schiff base was evaluated. Asp193 corresponds to Glu204 of bacteriorhodopsin (bR). The pK_a of the Schiff base (SBH^+) of D193N was ~10.1–10.0 (at XH^+) and ~11.4–11.6 (at X) depending on the protonation state of a certain residue (designated by X) and independent of Cl^-, whereas those of the wild type and D193E were >12. The pK_a values of XH^+ were ~11.8–11.2 at the state of SB, 10.5 at SBH^+ state in the presence of Cl^-, and 9.6 at SBH^+ without Cl^-. These imply the presence of a long-range interaction in the extracellular channel. Asp193 was suggested to be deprotonated in the present dodecylmaltoside (DDM) solubilized wild-type *p*pR, which is contrary to Glu204 of bR. In the absence of salts, the irreversible denaturation of D193N (but not the wild type and D193E) occurred via a metastable state, into which the addition of Cl^- reversed the intact pigment. This suggests that the negative charge at residue 193, which can be substituted by Cl^-, is necessary to maintain the proper conformation in the DDM-solubilized *p*pR.

INTRODUCTION

Sensory rhodopsin (sR or sensory rhodopsin I) (Bogomolni and Spudich, 1982; Hoff et al., 1997; Spudich et al., 2000) and phoborhodopsin (pR or sensory rhodopsin II, sRII) (Sasaki and Spudich, 2000; Takahashi et al., 1985; Zhang et al., 1996) are retinoid proteins of *Halobacterium salinarum* and work as photoreceptors; pR mediates the avoidance reaction from blue-green light. An alkali-halophilic bacterium, *Natronobacterium pharaonis*, also has a retinal pigment protein similar to pR, and it was purified and characterized in great detail (Chizhov et al., 1998; Engelhard et al., 1996; Hirayama et al., 1992, 1994, 1995; Miyazaki et al., 1992; Scharf et al., 1992; Seidel et al., 1995). This pigment was named *pharaonis* phoborhodopsin (*p*pR or *pharaonis* sensory rhodopsin II, psRII). It was reported that *p*pR is much more stable than pR. The functional expression of *p*pR in *Escherichia coli* has been achieved (Shimono et al., 1997), which yields large amounts of the protein that permits more detailed investigations. Recently, two groups solved the crystal structure of *p*pR (Luecke et al., 2001; Royant et al., 2001), thus opening the next stage of research for the photosensor.

The amino acid sequence of *p*pR (Seidel et al., 1995) is homologous to that of bacteriorhodopsin (bR), a well known light-driven proton pump (Lanyi, 2000; Oesterhelt and Stoeckenius, 1971). Important residues in the extracellular channel (EC) of bR (Asp85, Asp212, and Arg82) are all conserved in *p*pR as Asp75, Asp201, and Arg72, respectively, with the exception of Glu194, which is replaced by Pro183, and of Thr205, which is replaced by Val194 in *p*pR. Asp75 of *p*pR serves as a counterion of the protonated Schiff base (PSB or SBH^+) (Bergo et al., 2000; Engelhard et al., 1996). As mentioned above, two groups solved the crystal structure, and both showed that a side chain of Arg72 is oriented toward the extracellular side, which is a different orientation from bR. On the other hand, Asp96 in the cytoplasmic channel (CP) of bR is replaced by the neutral Phe86. Thr46, which is involved in tuning the pK_a of Asp96 in bR, is also missing. These replacements slow down the decay of the M-intermediate of *p*pR (Iwamoto et al., 1999a).

Upon absorption of a photon, *p*pR undergoes a photoreaction cycle (Chizhov et al., 1998; Hirayama et al., 1992; Miyazaki et al., 1992) similar to bR. Proton uptake and release during the photocycle of *p*pR have been detected (Iwamoto et al., 1999b), and the transmembranous proton transport from inside to outside was detected (Schmies et al., 2001, 2000; Sudo et al., 2001), although this activity was weak. Many studies of bR (Balashov et al., 1995, 1996, 1999; Brown et al., 1993, 1995, 1996; Dioumaev et al., 1998; Richter et al., 1996) have revealed the existence of a complex linkage from Glu204 to the Schiff base via its counterion Asp85 in EC. During the photocycle, this linkage cooperatively regulates the protonated state of these residues to achieve the prompt proton release. During the photocycling of *p*pR and pR, the proton uptake occurs first and then release occurs at the transition from the O-intermediate to the original *p*pR (Iwamoto et al., 1999b; Sasaki and Spudich, 1999); therefore, it is an important question as to whether an intramolecular linkage between the Schiff base and the outer surface of the protein exists in *p*pR as in bR.

In this study, we examined this problem. To this end, the pK_a of the PSB of the wild type, D193N, and D193E were determined. The presence of a negative charge at the 193-

Submitted January 9, 2002, and accepted for publication April 23, 2002.

H. Kandori's present address: Department of Applied Chemistry, Nagoya Institute of Technology, Showa-ku, Nagoya 466-8555, Japan.

Address reprint requests to Dr. Naoki Kamo, Laboratory of Biophysical Chemistry, Graduate School of Pharmaceutical Sciences, Hokkaido University, Sapporo 060-0812, Japan. Tel.: 81-11-7063923; Fax: 81-11-7064984; E-mail: nkamo@pharm.hokudai.ac.jp.

0006-3495/02/08/1130/06 $2.00

position increases the pK_a of the PSB by more than 2 units, indicating the existence of a long-range interaction. The existence of another protonatable residue affecting pK_a of the PSB is also suggested. In addition, the effects of the anion on the long-range interaction and the structural stability of D193N were investigated because Royant et al. (2001) presented the existence of Cl^- near Arg72 in their crystal structure of the wild-type *p*pR. The present study suggests that Cl^- may bind around Asp193 and that this bound Cl^- may play an important role both in maintaining the conformation and in regulating the pK_a of the PSB of D193N in which the negative charge at the 193-position is missing.

MATERIALS AND METHODS

Sample preparations

The expression of the histidine-tagged *p*pR in *E. coli* BL21(DE3) and its purification were described elsewhere (Hohenfeld et al., 1999). QuickChange site-directed mutagenesis kit (Stratagene, La Jolla, CA) was used to prepare D193N and the D193E mutant.

Spectroscopic analysis

The absorption spectra were taken using a model V-560 spectrophotometer (Jasco, Tokyo, Japan). The temperature was kept at 20°C. During the titration experiments for the absorption spectra of D193N, the pH was initially adjusted to 7.0 using a mixture of six buffers (containing citric acid, Mes, Hepes, Mops, Ches, and Caps, all concentrations of which were 10 mM each) and 0.1% DDM (*n*-dodecyl-β-D-maltoside). The pH titration of the PSB started from 7.0. The pH was adjusted to the desired value by the addition of concentrated NaOH, and the absorption spectra were then measured. Data fitting was done using Microcal Origin software (Microcal Software, Northampton, MA).

Chromophore extraction

The methods for the extraction and determination of the chromophore configuration were the same as described elsewhere (Shimono et al., 2001).

RESULTS

pH titration of the Schiff base in D193N

The spectroscopic titration of D193N was conducted. Fig. 1 shows the absorption spectra of D193N at various pH values from 7.0 to 12.7 in the presence of 200 mM NaCl. With an increase in the pH values, the absorption band at 360 nm due to the deprotonated Schiff base increased. Fig. 2 shows the titration curve of the PSB in D193N in the presence (Fig. 2 *a*) and absence (Fig. 2 *b*) of 200 mM NaCl. In the experiment in the absence of NaCl, 67 mM Na_2SO_4 was added so as to keep the ionic strength constant. When Na_2SO_4 was removed, the pKa values estimated below were essentially the same as those in the presence of Na_2SO_4. As described later, in a Cl^--free medium, D193N ($\lambda max \approx 500$ nm) gradually transforms into the metastable state ($\lambda max \approx 375$ nm) in ~10 h, and then during this period, the depletion of the 500-nm absorption by alkalization was analyzed as quickly as possible.

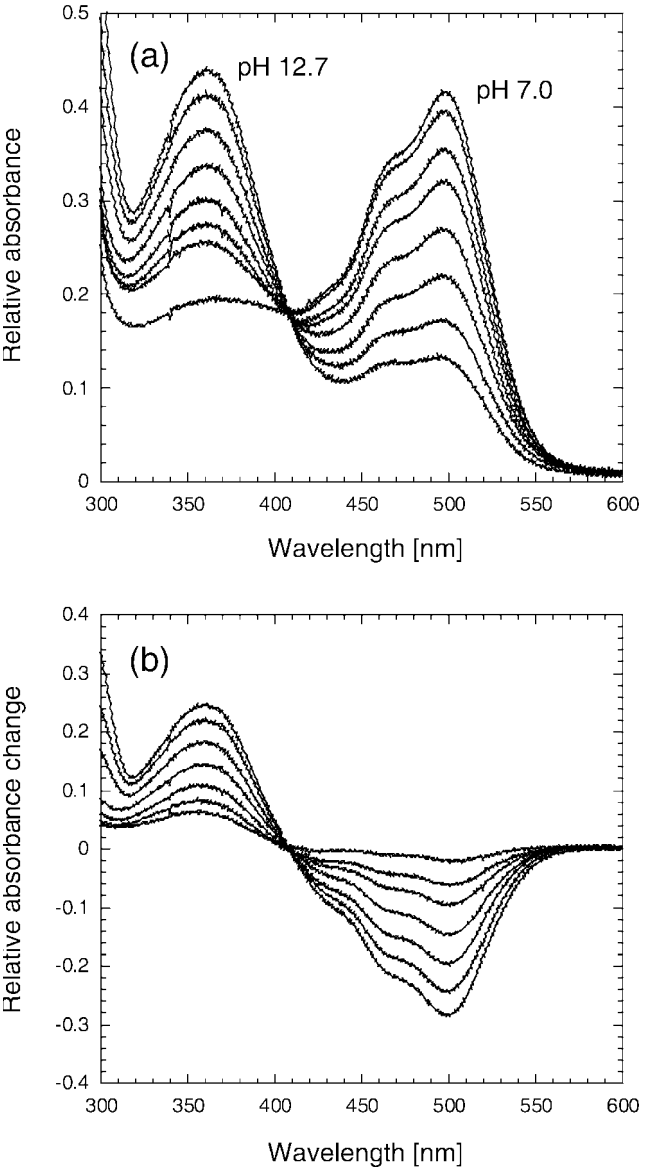

FIGURE 1 pH titration of the Schiff base in D193N in the presence of 200 mM NaCl. (*a*) Changes in absorption spectra of D193N from pH 7.0 to 12.7. pH values of each spectrum are 7.0, 9.5, 9.7, 9.9, 10.2, 11.3, 11.8, and 12.7, respectively. (*b*) Difference absorption spectra. Each spectrum was obtained by subtracting that of pH 7.0.

In contrast to the gecko cone-type visual pigment showing a large Cl^- dependence on the Schiff base pK_a (Yuan et al., 1999), the dependence was not great, but the deprotonation of the PSB in D193N exhibited a complex titration curve, indicative of the interaction by another protonatable residue. Thus, we fitted these titration curves with a model of two interacting residues (Balashov et al., 1995) (whose model is depicted in Fig. 2), and estimated pK_a values are listed in Table 1. The

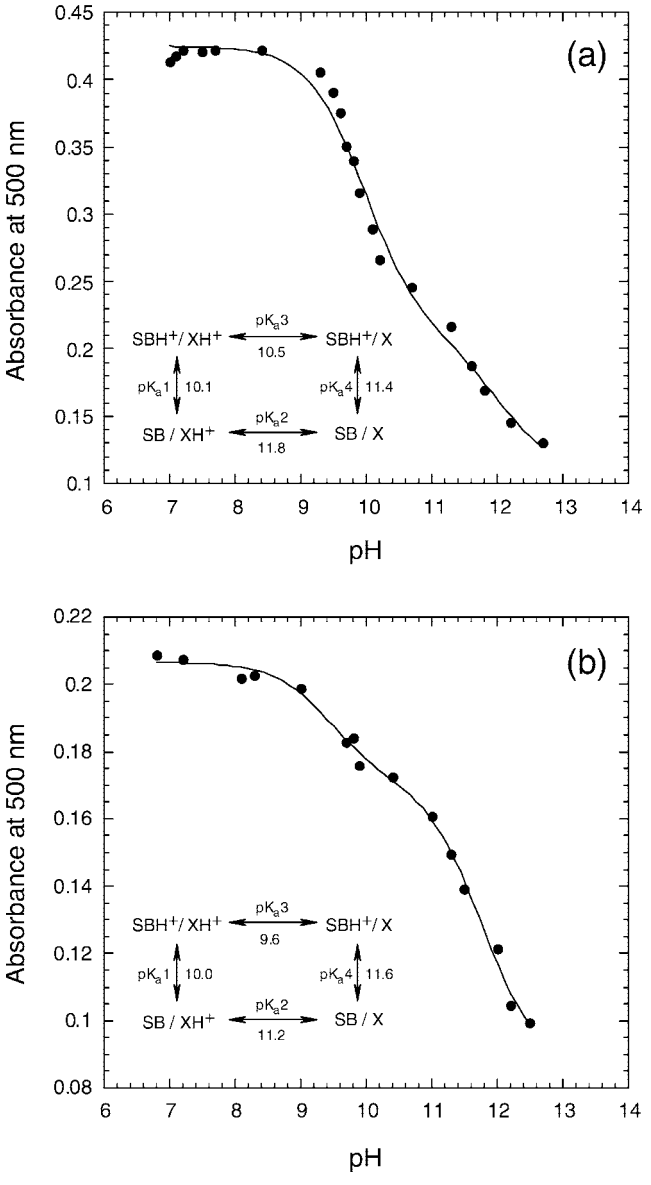

FIGURE 2 pH titration curves of the Schiff base in D193N. (*a*) In the presence of 200 mM Cl^-; (*b*) In a Cl-free medium (containing 67 mM Na_2SO_4 for keeping the ionic strength of 200 mM NaCl). Fitted curves were obtained with a model of two interacting residues (Balashov et al., 1995) which are shown in the panel. Residue X is an unknown protonatable residue whose protonation state affects the pK_a of the Schiff base.

pK_{a1} and pK_{a4} values are pK_a of the PSB when another protonatable residue (X) is protonated and deprotonated, respectively. The pK_{a2} and pK_{a3} values are pK_a of the X residue when the Schiff base is deprotonated and protonated, respectively. The pK_a of the PSB in the wild-type *p*pR was 12.4 (Balashov et al., in preparation) and no remarkable pK_a change in the PSB of D193E was observed (data not shown). On the other hand, that of D193N was lowered to 10.1 or 11.4, depending on whether residue X was protonated or deprotonated, respectively. Interestingly, the pK_a value of residue X was affected by Cl^- when the Schiff base is protonated (see pK_{a3} in Table 1), suggesting that the Cl^--binding site of D193N may locate near the X residue and that the negative charge of Cl^- may increase the pK_a of the X residue.

TABLE 1 pK_a values for titration of the Schiff base

	pK_{a1}	pK_{a2}	pK_{a3}	pK_{a4}
Wild-type	>12	–	–	–
D193N	10.1	11.8	10.5	11.4
D193N (Cl^- free)	10.0	11.2	9.6	11.6
D193E	>12	–	–	–

For the meanings of pK_i (i = 1–4), see Fig. 2.

Chromophore configuration

The chromophore configuration was examined in the presence of 200 mM NaCl and absence of Cl^- (i.e., 67 mM Na_2SO_4). The ratios of the all-*trans* retinal in the presence of Cl^- were 95.2%, 96.3%, and 90.8% for the wild type, D193E, and D193N, respectively, and they were, respectively, 94.0%, 87.7%, and 74.5% in the absence of Cl^-. The remainder was the 13-*cis* retinal. These were done in the dark because the titration experiments were done using the dark-adapted sample. The data shown in Fig. 2 may not be accountable by the idea of the difference in the Schiff base pK_a between the all-*trans* and 13-*cis* retinal, because the amplitudes of the components (shift amplitudes in the pH titration) obtained in Fig. 2 *a* cannot be explained by the molar ratio of the all-*trans* to 13-*cis* (~9:1).

Chloride effect on the stability of D193N

When the sample of D193N mutant was desalted at pH 7, a time-dependent decrease in the absorption peak at 498 nm and concomitant increase in the 375-nm peak was observed in the upper several tenths of an hour time range. These blue-shifted spectra reversed to normal when Cl^- was added to the sample. Fig. 3 shows the recovery of the absorbance at 498 nm with an isosbestic point of 420 nm by adding NaCl to the desalted D193N sample. The spectral shoulder at around 460 nm that is characteristic of *p*pR and pR also recovered with the recovery of the 498-nm absorbance. It should be stressed that no blue shift was observed for the desalted samples of both the wild type (Shimono et al., 2000) and D193E (data not shown), suggesting that the blue shift and the recovery by Cl^- are observed only for a mutant of D193N that lacks the negative charge at the 193 positions.

After the desalted D193N sample was left for a longer time (e.g., several days or a week), the extent of recovery of the

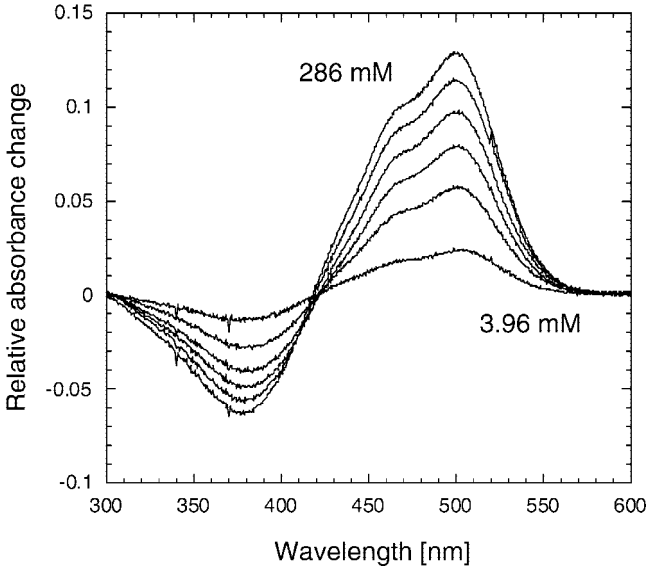

FIGURE 3 Difference absorption spectra by adding NaCl to the desalted sample of D193N. Cl^- concentrations are 3.96, 7.84, 13.5, 24.4, 79.6, and 286 mM, respectively. The pH was 7.0

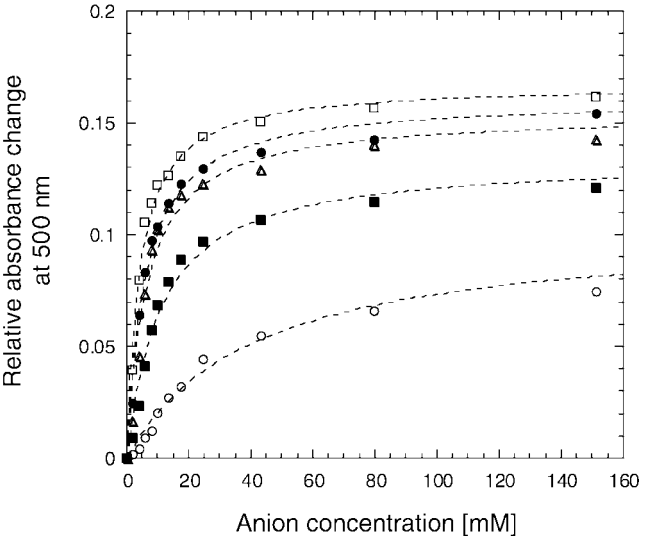

FIGURE 4 Anion binding to D193N detected by measuring absorbance change at 500 nm. Absorbance at 280 nm of each spectrum was adjusted to 1, and absorbance changes at 500 nm by adding anions were plotted. Dotted curves are the best fitted curves of each plot to Michaelis-Menten equation. ○, data set of F^-; ■, Cl^-; △, Br^-; □, I^-; ●, NO_3^-.

absorbance at 498 nm by NaCl was significantly decreased. Therefore, one may consider the following scheme:

$$\text{D193N} \underset{\text{Cl}^-}{\overset{\text{deionized}}{\rightleftharpoons}} \text{metastable state } (\lambda_{max} \sim 375 \text{ nm})$$

$$\xrightarrow{\text{very slow}} \text{irreversibly denatured state}$$

The absorption maximum of the metastable state might suggest the de-protonated Schiff base species, but this is not the case because the pK_a of the PSB of D193N in the absence of Cl^- was 10.0 or 11.6 depending on the protonation state of the X residue (see Table 1). The addition of Cl^- to the metastable state resumed the intact D193N, suggesting that retinal is not liberated from the protein. The absorption maximum of retinal forming the Schiff base in solutions is ~380 nm. In the metastable state, hence, the protein conformation might become looser than that of the stable state and the retinal in the protein moiety might be surrounded by water.

Effect of various anions

To examine whether the recovery from the metastable state to the normal D193N specific to Cl^-, various anions were added to the metastable state. In Fig. 4, the increases in the absorbance at 500 nm are plotted as a function of various anion concentrations, showing that not only chloride but also other halogen ions or the nitrate ion have the ability for recovery from the metastable state. From these results, the apparent Kd values of each anion were calculated by fitting using the Michaelis-Menten equation. These values are 43.3 ± 4.4 mM for F^-, 11.0 ± 1.2 mM for Cl^-, 6.4 ± 0.9 mM for Br^-, 4.2 ± 0.3 mM for I^-, and 5.9 ± 0.5 mM for NO_3^-. The order of the 1/Kd values for various anions is interestingly the same as that known as the Hofmeister series that represents the order of the hydrophobicity and the tendency to stabilize structured low-density water of anions.

DISCUSSION

Asp193 of the DDM-solubilized wild type may be deprotonated at pH 7 in the ground state

Figs. 3 and 4 imply that for D193N, the anion may bind to the interior of protein and this binding is needed for maintaining the correct conformation. The anion order of the potency to maintain a suitable conformation is the same as the Hofmeister series, suggesting a relatively hydrophobic or the low-density water structured binding site. The wild type and D193E of *p*pR were not converted to the metastable state even in the absence of Cl^- in contrast to D193N. This may lead to the hypothesis that the position at 193 bears the negative charge for the wild type or D193E from neutral to alkaline (which is the pH range in the present experiment) and that for D193N, Cl^- may substitute for this negative charge. This also implies that the binding site of the anion may not be far from the 193-position, at least for D193N.

The pK_{a1} shown in Table 1 also supports the deprotonation of Asp193 of the wild type or D193E at pH 7. It is worth noting, therefore, that Asp193 of the DDM-solubilized *p*pR is deprotonated at pH 7.0 whereas Glu204 of bR corresponding to Asp193 of *p*pR is presumably protonated,

whose pK_a at the ground state is estimated at ~10 (Balashov et al., 1995, 1996, 1999). However, our preliminary results from the low-temperature FTIR suggest that Asp193 is protonated at pH 5–7 (Furutani et al., in preparation). It is noted that the FTIR sample was incorporated into the liposomes. Therefore, the apparent contradiction may be explained as follows: 1) Asp193 in the present DDM-solubilized sample may be partially protonated at pH 7 or 2) its pK_a may increase when the protein is embedded into lipids whereas Asp193 of this solubilized sample dissociates mostly. At present, we do not know which is correct. Nevertheless, it is obvious that there is a significant difference in the pK_a of Asp193 (*p*pR) and Glu204 (bR).

This difference may be reflected by the difference in fine structure of the EC channel between *p*pR and bR. The crystal structure of *p*pR (Luecke et al., 2001; Royant et al., 2001) recently reported shows some differences from bR, particularly the difference in the orientation of Arg72, the side chain of which faces the extracellular side whereas Arg82 of bR relatively faces to the Schiff base; i.e., the distance of each guanidinium nitrogen atoms of the Arg72 from the Schiff base in *p*pR is ~11 Å whereas that of one guanidinium nitrogen atom of Arg82 is ~8 Å in bR. It might be possible to consider that this different orientation of the positive charge gives rise to the pK_a difference between Asp193 of *p*pR and Glu204 of bR. Another candidate for this reason may be the lack of the carboxyl group at residue 183 (Pro183) whose position corresponds to Glu194 of bR. As mentioned above, the proton uptake and release of *p*pR (Iwamoto et al., 1999b) resemble the bR mutants (Brown et al., 1995; Koyama et al., 1998) whose proton-releasing complex (PRC) is incomplete. The deprotonation of Asp193 might be one of the reasons that when compared with bR, there is a much longer delay of the proton release after the proton transfer from the PSB to its counterion. It is indispensable for further research to estimate the pK_a value of Asp193 in the wild-type *p*pR.

pK_a of the Schiff base in D193N

This value was estimated to be ~10 whereas that of the wild type or D193E was ~12, suggesting that the negative charge at the 193-position increases the proton affinity of the Schiff base in the wild-type *p*pR. Referring to the recent crystal structure of *p*pR (Luecke et al., 2001; Royant et al., 2001), the distance between the Schiff base and the side chain of Asp193 is ~14 Å. Therefore, the existence of the long-range interaction, like the hydrogen-bonding network between the Schiff base and the extracellular surface of the protein revealed in bR, is expected. If this interaction exists, the pK_a shifts of the Schiff base and Asp75 (the counterion of the PSB) might be observed in the Arg72 *p*pR mutant as is similar to the R82A bR mutant (Balashov et al., 1993). The effect of the Arg residue on these pK_a values is now in progress.

Another interesting point is the existence of a protonatable residue whose protonation states affect the pK_a of the Schiff base. A possible candidate for this protonatable residue is Arg72 judging from the location within the EC channel and from its pK_a value; Arg72 guanidinium of *p*pR locates ~11 Å from the Schiff base and ~5 Å from Asp193 carboxyl, and the estimated pK_a of residue X (see Fig. 2) resembles that of Arg (11.8 or 10.5 when the Schiff base is deprotonated or protonated, respectively) although the pK_a value is somewhat smaller than the usual value. In addition, our results show that Cl^- mainly affects the pK_a not of the Schiff base (pK_{a1} and pK_{a4}) but of residue X when the Schiff base is protonated. The change in the pK_a is due presumably to the electrostatic interaction (pK_{a2} and pK_{a3}; see Fig. 2 and Table 1). This might indicate that in the D193N mutant, the Cl^--binding site is close to residue X, presumably Arg72. Royant et al. (2001) proposed the existence of the Cl^--binding site in addition to several water molecules near Arg72 in the wild-type *p*pR, and then it is probable that this site might be the anion-binding site, which is proved in the D193N mutant in the present paper. The conclusion whether the Cl-binding site exists in the wild type must await further studies. In any case, it may be certain that for the D193N mutant, the same bound Cl^- has a role in both the regulation of the pK_a values and maintenance of the proper conformation.

Concluding remarks

The present investigation revealed the existence of a long-range interaction that extended from the extracellular surface to the Schiff base in *p*pR. Water molecules may be involved in this interaction as is proved in bR. Thus, cooperative linkages among the amino acid residues and water molecules in the EC channel via hydrogen bonding would be a common feature of the archaeal retinal proteins. How is this network involved in their function? In addition, why is the proton release delayed in the case of the *p*pR despite the organized linkage of EC? These questions must be considered in a further study.

This work was supported by Research Fellowships from the Japan Society for the Promotion of Science for Young Scientists, and by Grants-in-aid for Scientific Research from the Japanese Ministry of Education, Science, Sports, and Culture.

REFERENCES

Balashov, S. P., R. Govindjee, E. S. Imasheva, S. Misra, T. G. Ebrey, Y. Feng, R. K. Crouch abd D. R. Menick. 1995. The two pKa's of aspartate-85 and control of thermal isomerization and proton release in the arginine-82 to lysine mutant of bacteriorhodopsin. *Biochemistry.* 34:8820–8834.

Balashov, S. P., R. Govindjee, M. Kono, E. Imasheva, E. Lukashev, T. G. Ebrey, R. K. Crouch, D. R. Menick, and Y. Feng. 1993. Effect of the arginine-82 to alanine mutation in bacteriorhodopsin on dark adaptation, proton release and photochemical cycle. *Biochemistry.* 32:10331–10343.

Balashov, S. P., E. S. Imasheva, R. Govindjee, and T. G. Ebrey. 1996. Titration of aspartate-85 in bacteriorhodopsin: what it says about chromophore isomerization and proton release. *Biophys. J.* 70:473–481.

Balashov, S. P., M. Lu, E. S. Imasheva, R. Govindjee, T. G. Ebrey, B. Othersen, Y. Chen, R. K. Crouch, and D. R. Menick. 1999. The proton release group of bacteriorhodopsin controls the rate of the final step of its photocycle at low pH. *Biochemistry.* 38:2026–2039.

Bergo, V., E. N. Spudich, K. L. Scott, J. L. Spudich, and K. J. Rothschild. 2000. FTIR analysis of the SII540 intermediate of sensory rhodopsin II: Asp73 is the Schiff base proton acceptor. *Biochemistry.* 39:2823–2830.

Bogomolni, R. A., and J. L. Spudich. 1982. Identification of a third rhodopsin-like pigment in phototactic *Halobacterium halobium. Proc. Natl. Acad. Sci. U.S.A.* 79:6250–6254.

Brown, L. S., L. Bonet, R. Needleman, and J. K. Lanyi. 1993. Estimated acid dissociation constants of the Schiff base, Asp-85, and Arg-82 during the bacteriorhodopsin photocycle. *Biophys. J.* 65:124–130.

Brown, L. S., R. Needleman, and J. K. Lanyi. 1996. Interaction of proton and chloride transfer pathways in recombinant bacteriorhodopsin with chloride transport activity: implications for the chloride translocation mechanism. *Biochemistry.* 35:16048–16054.

Brown, L. S., J. Sasaki, H. Kandori, A. Maeda, R. Needleman, and J. K. Lanyi. 1995. Glutamic acid 204 is the terminal proton release group at the extracellular surface of bacteriorhodopsin. *J. Biol. Chem.* 270: 27122–27126.

Chizhov, I., G. Schmies, R. Seidel, J. R. Sydor, B. Lüttenberg, and M. Engelhard. 1998. The photophobic receptor from *Natronobacterium pharaonis*: temperature and pH dependencies of the photocycle of sensory rhodopsin II. *Biophys. J.* 75:999–1009.

Dioumaev, A. K., H. T. Richter, L. S. Brown, M. Tanio, S. Tuzi, H. Saito, Y. Kimura, R. Needleman, and J. K. Lanyi. 1998. Existence of a proton transfer chain in bacteriorhodopsin: participation of Glu-194 in the release of protons to the extracellular surface. *Biochemistry.* 37: 2496–2506.

Engelhard, M., B. Scharf, and F. Siebert. 1996. Protonation changes during the photocycle of sensory rhodopsin II from *Natronobacterium pharaonis. FEBS Lett.* 395:195–198.

Hirayama, J., Y. Imamoto, Y. Shichida, N. Kamo, H. Tomioka, and T. Yoshizawa. 1992. Photocycle of phoborhodopsin from haloalkaliphilic bacterium (*Natronobacterium pharaonis*) studied by low-temperature spectrophotometry. *Biochemistry.* 31:2093–2098.

Hirayama, J., Y. Imamoto, Y. Shichida, T. Yoshizawa, A. E. Asato, R. S. Liu, and N. Kamo. 1994. Shape of the chromophore binding site in *pharaonis* phoborhodopsin from a study using retinal analogs. *Photochem. Photobiol.* 60:388–393.

Hirayama, J., N. Kamo, Y. Imamoto, Y. Shichida, and T. Yoshizawa. 1995. Reason for the lack of light-dark adaptation in *pharaonis* phoborhodopsin: reconstitution with 13-cis-retinal. *FEBS Lett.* 364:168–170.

Hoff, W. D., K. H. Jung, and J. L. Spudich. 1997. Molecular mechanism of photosignaling by archaeal sensory rhodopsins. *Annu. Rev. Biophys. Biomol. Struct.* 26:223–258.

Hohenfeld, I. P., A. A. Wegener, and M. Engelhard. 1999. Purification of histidine tagged bacteriorhodopsin, *pharaonis* halorhodopsin and *pharaonis* sensory rhodopsin II functionally expressed in *Escherichia coli. FEBS Lett.* 442:198–202.

Iwamoto, M., K. Shimono, M. Sumi, and N. Kamo. 1999a. Positioning proton-donating residues to the Schiff-base accelerates the M-decay of *pharaonis* phoborhodopsin expressed in *Escherichia coli. Biophys. Chem.* 79:187–192.

Iwamoto, M., K. Shimono, M. Sumi, K. Koyama, and N. Kamo. 1999b. Light-induced proton uptake and release of *pharaonis* phoborhodopsin detected by a photoelectrochemical cell. *J. Phys. Chem. B.* 103: 10311–10315.

Koyama, K., T. Miyasaka, R. Needleman, and J. K. Lanyi. 1998. Photoelectrochemical verification of proton-releasing groups in bacteriorhodopsin. *Photochem. Photobiol.* 68:400–406.

Lanyi, J. K. 2000. Molecular mechanism of ion transport in bacteriorhodopsin: insights from crystallographic, spectroscopic, kinetic, and mutational studies. *J. Phys. Chem. B.* 104:11441–11448.

Luecke, H., B. Schobert, J. K. Lanyi, E. N. Spudich, and J. L. Spudich. 2001. Crystal structure of sensory rhodopsin II at 2.4 angstroms: insights into color tuning and transducer interaction. *Science.* 293:1499–1503.

Miyazaki, M., J. Hirayama, M. Hayakawa, and N. Kamo. 1992. Flash photolysis study on *pharaonis* phoborhodopsin from a haloalkaliphilic bacterium (*Natronobacterium pharaonis*). *Biochim. Biophys. Acta.* 1140:22–29.

Oesterhelt, D., and W. Stoeckenius. 1971. Rhodopsin-like protein from the purple membrane of *Halobacterium halobium. Nat. New Biol.* 233: 149–152.

Richter, H. T., L. S. Brown, R. Needleman, and J. K. Lanyi. 1996. A linkage of the pKa's of asp-85 and glu-204 forms part of the reprotonation switch of bacteriorhodopsin. *Biochemistry.* 35:4054–4062.

Royant, A., P. Nollert, K. Edman, R. Neutze, E. M. Landau, E. Pebay-Peyroula, and J. Navarro. 2001. X-ray structure of sensory rhodopsin II at 2.1-Å resolution. *Proc. Natl. Acad. Sci. U.S.A.* 98:10131–10136.

Sasaki, J., and J. L. Spudich. 1999. Proton circulation during the photocycle of sensory rhodopsin II. *Biophys. J.* 77:2154–2152.

Sasaki, J., and J. L. Spudich. 2000. Proton transport by sensory rhodopsins and its modulation by transducer binding. *Biochim. Biophys. Acta.* 1460:230–239.

Scharf, B., B. Pevec, B. Hess, and M. Engelhard. 1992. Biochemical and photochemical properties of the photophobic receptors from *Halobacterium halobium* and *Natronobacterium pharaonis. Eur. J. Biochem.* 206:359–366.

Schmies, G., M. Engelhard, P. G. Wood, G. Nagel, and E. Bamberg. 2001. Electrophysiological characterization of specific interactions between bacterial sensory rhodopsins and their transducers. *Proc. Natl. Acad. Sci. U.S.A.* 98:1555–1559.

Schmies, G., B. Lüttenberg, I. Chizhov, M. Engelhard, A. Becker, and E. Bamberg. 2000. Sensory rhodopsin II from the haloalkaliphilic *Natronobacterium pharaonis*: light-activated proton transfer reaction. *Biophys. J.* 78:967–976.

Seidel, R., B. Scharf, M. Gautel, K. Kleine, D. Oesterhelt, and M. Engelhard. 1995. The primary structure of sensory rhodopsin II: a member of an additional retinal protein subgroup is coexpressed with its transducer, the halobacterial transducer of rhodopsin II. *Proc. Natl. Acad. Sci. U.S.A.* 92:3036–3040.

Shimono, K., M. Iwamoto, M. Sumi, and N. Kamo. 1997. Functional expression of *pharaonis* phoborhodopsin in *Escherichia coli. FEBS Lett.* 420:54–56.

Shimono, K., Y. Ikemura, Y. Sudo, M. Iwamoto, and N. Kamo. 2001. Environment around the chromophore in *pharaonis* phoborhodopsin: mutation analysis of the retinal binding site. *Biochim. Biophys. Acta.* 1515:92–100.

Shimono, K., M. Kitami, M. Iwamoto, and N. Kamo. 2000. Involvement of two groups in reversal of the bathochromic shift of *pharaonis* phoborhodopsin by chloride at low pH. *Biophys. Chem.* 87:225–230.

Spudich, J. L., C. S. Yang, K. H. Jung, and E. N. Spudich. 2000. Retinylidene proteins: structures and functions from archaea to humans. *Annu. Rev. Cell Dev. Biol.* 16:365–392.

Sudo, Y., M. Iwamoto, K. Shimono, M. Sumi, and N. Kamo. 2001. Photo-induced proton transport of *pharaonis* phoborhodopsin (sensory rhodopsin II) is ceased by association with the transducer. *Biophys. J.* 80:916–922.

Takahashi, T., H. Tomioka, N. Kamo, and Y. Kobatake. 1985. A photosystem other than PS370 also mediates the negative phototaxis of *Halobacterium halobium. FEMS Microbiol. Lett.* 28:161–164.

Yuan, C., O. Kuwata, J. Liang, S. Misra, S. P. Balashov, and T. G. Ebrey. 1999. Chloride binding regulates the Schiff base pKa in gecko P521 cone-type visual pigment. *Biochemistry.* 38:4649–4654.

Zhang, W., A. Brooun, M. M. Mueller, and M. Alam. 1996. The primary structures of the archaeon *Halobacterium salinarium* blue light receptor sensory rhodopsin II and its transducer, a methyl-accepting protein. *Proc. Natl. Acad. Sci. U.S.A.* 93:8230–8235.